JOURNAL OF MATERIALS SCIENCE 24 (1989) 2939–2950

Polyamide 6/ethylene–vinyl acetate copolymer blends: melt rheology and morphology of extruded samples

M. L. ADDONIZIO, L. D'ORAZIO, C. MANCARELLA, E. MARTUSCELLI
Istituto di Ricerche su Tecnologia dei Polimeri e Reologia del C.N.R., Via Toiano 6, 80072 Arco Felice, Napoli, Italy

A. CASALE, A. FILIPPI
Tecnopolimeri S.p.A., Ceriano Laghetto, Milano, Italy

A study of the rheological behaviour of polyamide 6 (PA6) and PA6/ethylene–vinyl acetate copolymers (EVA) blends in the molten state is reported. Zero shear viscosity, η_0, and the activation energy for the viscous flow, ΔE^*, were obtained as functions of both composition and molar mass of the components. The mode and state of dispersion of the minor components in samples of extruded blends were extensively analysed and correlated with molecular characteristics and chemical structure of the EVA copolymers.

1. Introduction

In our previous paper [1] we presented the results of an investigation concerning mainly the study of the influence of composition and post-blending processing conditions on the rheological behaviour and on the morphology of blends of Nylon 6 (PA6) with an ethylene–vinyl acetate copolymer (EVA). Extrudate materials were processed according to two different methods: capillary extrusion at very low shear rate and injection moulding at 220, 240 and 260° C with three different residence times. The capillary rheometer was also employed for determining the rheological properties of the pure homopolymers and blends. It was found that, for a given shear stress and residence temperature the apparent viscosity (η_a) of the blends is lower than that of PA6 and decreases with increasing the EVA content; no systematic dependence of such η_a values upon residence time was observed.

In the case of blends extruded through the capillary, scanning electron microscopy (SEM), coupled with an etching technique, based on selective EVA dissolution, had shown that blend composition played a predominant role in determining which one of the two components forms the dispersed and which ones the continuous phase.

The mode and the state of dispersion of the minor component were found to be controlled by both composition and extrusion temperature. It is interesting to note that at the blend composition PA6/EVA 40/60 the copolymer represented the continuous phase including the polyamide as the dispersed one. The PA6 domains which resulted were, moreover, elongated along the extrusion direction [1] giving rise to a true molecular composite. It should be stressed that at low extrusion temperature and also the residence time became relevant factors in affecting dispersed phase morphology [1].

For the injection-moulded samples, it was observed that the processing temperature and/or the residence time do not influence the mode and state of dispersion of the minor component. The average particle size of the EVA domains was found to increase with increasing copolymer content. From a study performed on the correlations between phase morphology and impact behaviour of the injection-moulded samples it appears that the success in improving the impact properties of PA6 depend mainly on the ability to control the EVA particle size and/or to increase interfacial interactions.

In a second paper [2], dealing with PA6/EVA system, we reported the properties of injection-moulded blends of PA6 with various samples of EVA copolymers differing in vinyl acetate content, molecular mass and melt viscosity. Blends of PA6 with a sample of ethylene–vinyl acetate–acrylic acid terpolymer were also investigated in order to assess the influence of carboxylic pendant groups on the interfacial interactions between dispersed phase and PA6 matrix.

The analysis by SEM of the mode and state of dispersion of the minor component showed that the processing induced an anisotropic distribution of the dispersed phase with the presence of a skin layer almost free of the minor component. It was found that on moving from the surface towards the core of the specimen the concentration of the copolymer increases.

A segregation of the dispersed phase in spherical-shaped domains was observed. The average particle size resulted to be dependent on the molecular characteristics of the EVA used. According to Chang Dae Han and Hsiao-Ken Chuang [3, 4], no evidence of chemical reaction between PA6 and EVA was observed. The mode and fracture mechanism of the injection-moulded PA6/EVA blends were found to be determined by a combination of shear yielding and

0022–2461/89 $03.00 + .12

multiple craze formation mechanisms. The amount of such processes and how they interact tended to be dependent mainly on the average particle size of the dispersed phase. Better impact behaviour was shown by blends for which lower dimensions of dispersed particles were measured. The degree of adhesion seemed to play only a secondary role in conferring toughening in polyamide, in agreement with the results obtained by Wu [5].

From our studies aimed at correlating overall morphology developed in the injection-moulding process with impact properties of PA6/EVA blends, we concluded that in such incompatible polymer blends the mechanical response is determined by a combination of interrelated factors such as phase viscosity ratio, molecular mass, molecular mass distribution and molecular structure of EVA copolymers, as well as blend composition. The goal of the research reported in the present paper, was to optimise some of the factors identified above, keeping the others almost constant. To attain this aim, we blended PA6 with several EVA copolymers differing in molecular mass and for a given molecular mass in the vinyl acetate content (from 20% up to 40% (wt/wt)).

The melt rheology and the overall morphology developed in samples of extruded PA6-based blends containing 10% (wt/wt) of each copolymer were then investigated. The mode and state of dispersion of the minor component was correlated with its own molecular mass and molecular structure. The final target of the research is to tailor the phase morphology of PA6/EVA blends and then the ultimate properties of the blend material.

2. Materials and methods

2.1. Materials and blending

The materials used in this study were Nylon 6 (PA6, Snia) with a number average molecular weight ($\bar{M}_n$) of 18 000, and seven different commercial ethylene–vinyl acetate copolymers (EVA). The codes of the copolymers, the weight percentage of vinyl acetate, the melt flow index, the observed melting temperature (T'_m) and the glass transition temperature (T_g) are listed in Table I.

The blends, all containing 10 wt % EVA, were obtained by extruding the two components in a double-screw extruder (Creusot-Loire diameter = 56 mm) operating at 83 r.p.m. and at a temperature of 240° C.

TABLE I Molecular characteristics, glass transition (T_g) and observed melting temperatures (T'_m) of the plain polyamide 6 (PA6) and the ethylene–vinyl acetate copolymers (EVA)

Code	% vinyl acetate (wt/wt)	Melt index (MI) (g 10 min^{-1})	T_g (°C)	T'_m (°C)
PA6	–	–	48	226
EVA1	20	300–500	−19	80
EVA2	20	3–4	−15	88
EVA3	30	300–500	−19	60
EVA4	30	30–40	−17	60
EVA5	30	3–4	−15	63
EVA6	35	30–40	−16	53
EVA7	40	30–40	−15	55

2.2. Sample preparation and techniques

Before examining, the extrudate materials in the form of cylindrical filaments (about 2 mm diameter), were water conditioned following a procedure described elsewhere [6].

Apparent viscosities were obtained, for a suitable range of temperatures (230, 240, 250 and 260° C) using a capillary rheometer (Gottfert HKR 2000) equipped with a pressure transmitter. The samples were forced through a capillary of radius 0.5 mm and length 30 mm under an applied pressure ranging between 5×10^7 and 80×10^7 dyn cm^{-2}. The shear rates at the walls, $\dot{\gamma}$, were measured at a given temperature.

The overall morphology of the extrudate blends was investigated by means of optical and scanning electron microscopy (SEM). Optical micrographs of thin cross-sections (about 10 μm thick) of the filaments were taken by using a Leitz optical polarizing microscope. The cryogenical fracture surfaces of the filaments were observed by means of an SEM 501 Philips after coating with gold–palladium. In order better to elucidate the mode and state of dispersion of the EVA copolymer into the PA6, a selective copolymer dissolution by means of xylene was carried out on smoothed transverse surfaces of the filaments. The resulting etched surfaces were subsequently prepared for SEM investigation. It has already been observed that the EVA copolymers were easily dissolved by xylene, whereas the PA6 remained unaffected [1].

The glass transition temperatures (T_g), the observed melting temperatures (T'_m) and the crystallinity index of pure PA6 and its blends with EVA copolymers were obtained using a differential scanning calorimeter (DSC) Mettler TA 3000. The following procedure was used: the samples of copolymers (about 20 mg) were heated from −100° C up to 150° C while the samples of pure PA6 and PA6/EVA blends (about 20 mg) were heated from −100° C up to 300° C at a rate of 20° C min^{-1}, and the heat (dH/dt) evolved during the scanning process was recorded as a function of temperature. T_g was taken as the temperature corresponding to 50% transition. The observed melting temperature T'_m and the apparent enthalpies of fusion, ΔH^*, were obtained from flex point and area of the melting peaks, respectively. The glass transition (T_g) of the plain PA6 and starting EVA copolymers are reported in Table I. In agreement with literature data [7] the T_g of PA6 is found at about 48° C. The T_g of EVA copolymers is found to be almost independent of the percentage of vinyl acetate. A slight decrease in the T_g values with decreasing molecular mass of the copolymers containing the same percentage of vinyl acetate is observed (see Table I).

The crystallinity index of PA6 phase (X_c(PA6)) and of overall blend (X_c(blend)) was calculated by means of the following relations:

$$X_c(\text{PA6}) = \frac{\Delta H^*(\text{PA6})}{\Delta H^0(\text{PA6})} \quad X_c(\text{blend}) = \frac{\Delta H^*(\text{blend})}{\Delta H^0(\text{PA6})}$$

where ΔH^*(PA6) is the apparent enthalpy of fusion per gram of PA6 in the blend; ΔH^0(PA6) is the heat of fusion per gram of 100% crystalline PA6 (from [8]

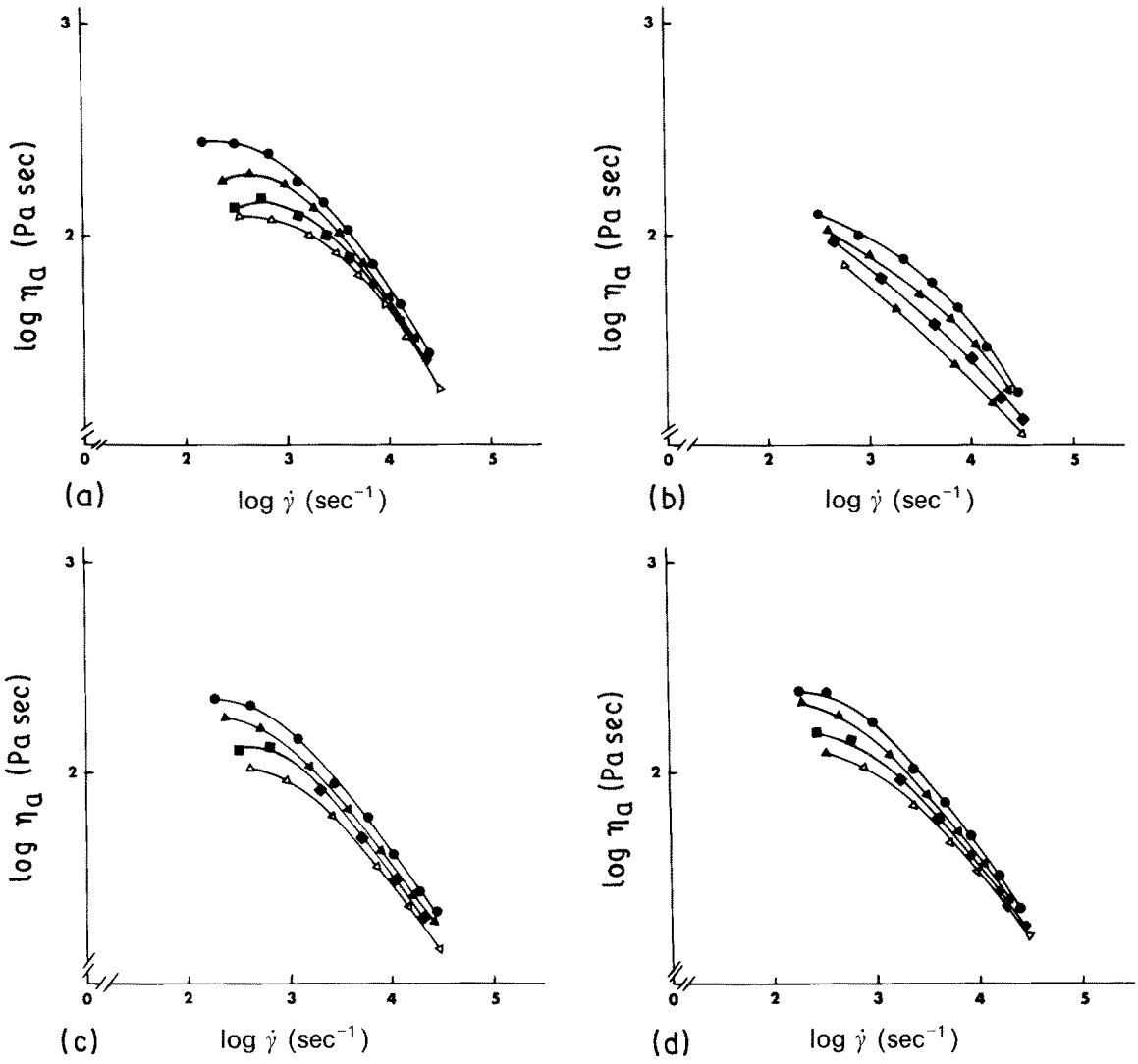

Figure 1 Typical dependence of the logarithm of the apparent viscosity, η_a, on the logarithm of shear rate, $\dot{\gamma}$, for (a) plain PA6 and (b) PA6/EVA3 (90/10), (c) PA6/EVA4 (90/10) and (d) PA6/EVA5 (90/10) blends: (●) 230° C, (▲) 240° C, (■) 250° C, (△) 260° C.

ΔH^0(PA6) = 188 J g^{-1}) and ΔH^*(blend) is the apparent enthalpy of fusion per gram of blend.

3. Results and discussion

3.1. Thermal behaviour and crystallinity

The DSC thermograms of plain PA6 show multiple fusion peaks. In Tables I and II the PA6 melting temperatures corresponding to the highest temperature peaks are reported. It seems reasonable to suppose that such temperatures are characteristic of the melting of the more stable α crystalline form of the PA6 [9].

TABLE II Observed melting temperatures (T'_m) of plain PA6 and PA6 crystallized from its blends with EVA copolymers together with crystallinity index of PA6 phase (X_c(PA6)) and PA6/EVA blends (X_c(blend)). The error on T'_m values is ±1° C

Code	T'_m (° C)	X_c(blend) (%)	X_c(PA6) (%)
PA6	218	–	28
PA6/EVA1	218	24	27
PA6/EVA2	218	24	27
PA6/EVA3	218	25	28
PA6/EVA4	217	25	28
PA6/EVA5	218	25	28
PA6/EVA6	218	24	27
PA6/EVA7	217	24	27

The thermograms of EVA copolymers show the presence of endothermic peaks due to the melting of ethylene blocks; the corresponding temperatures are reported in Table I. As shown, the T'_m values are found to be dependent on both the vinyl acetate content and molecular mass of the copolymers. T'_m values in fact decrease strongly with increasing vinyl acetate percentage (wt/wt) along the copolymer chain. Compare T'_m values of EVA1 and EVA2 copolymers with T'_m values of EVA6 and EVA7 copolymers. Looking at the T'_m values of those copolymers containing the same amount of vinyl acetate, an expected increase in the T'_m values with increasing molecular mass was found.

The DSC thermograms of PA6/EVA extruded blends show multiple fusion peaks probably due to recrystallization phenomena in the course of heating and polymorphic transition. Because of the difficult resolution of such peaks, the crystallinity index of the PA6 (X_c(PA6)) and the blends (X_c(blend)) was determined as follows: the samples (about 20 mg) were melted at a rate of 20° C min^{-1}, kept at 300° C for 3 min, cooled at a rate of 20° C min^{-1} and remelted at a rate of 20° C min^{-1}. The T'_m and X_c values thus obtained for the plain PA6 and PA6/EVA blends are reported in Table II. As shown, the T'_m values of PA6 crystallized from its blends with EVA copolymers

TABLE III Zero-shear viscosity, η_0, and parameter, α, calculated from Equation 1 for plain polyamide 6 (PA6) and PA6/ethylene–vinyl acetate copolymer (EVA) blends as function of the temperatures investigated

T (°C)	MI = 300–500						MI = 30–40						MI = 3–4			
	PA6 100%		PA6/EVA1		PA6/EVA3		PA6/EVA4		PA6/EVA6		PA6/EVA7		PA6/EVA2		PA6/EVA5	
	η_0 (Pa sec)	α (10^{-3} sec)	η_0 (Pa sec)	α (10^{-3} sec)	η_0 (Pa sec)	α (10^{-3} sec)	η_0 (Pa sec)	α (10^{-3} sec)	η_0 (Pa sec)	α (10^{-3} sec)	η_0 (Pa sec)	α (10^{-3} sec)	η_0 (Pa sec)	α (10^{-3} sec)	η_0 (Pa sec)	α (10^{-3} sec)
230	347.2	0.646	212.8	1.19	266.7	1.78	534.1	4.23	626.3	6.08	1043.3	10.27	618.5	4.99	729.3	6.61
240	247.4	0.477	140.9	0.820	177.0	1.10	433.2	3.83	395.6	3.30	549.3	5.77	401.8	2.91	441.6	3.39
250	182.6	0.336	105.3	0.664	137.4	0.950	290.2	2.29	338.0	3.32	386.9	3.79	265.3	1.75	339.2	2.62
260	159.0	0.307	78.1	0.609	104.5	0.841	239.6	2.08	225.3	1.96	229.9	1.80	164.2	0.923	221.6	1.42

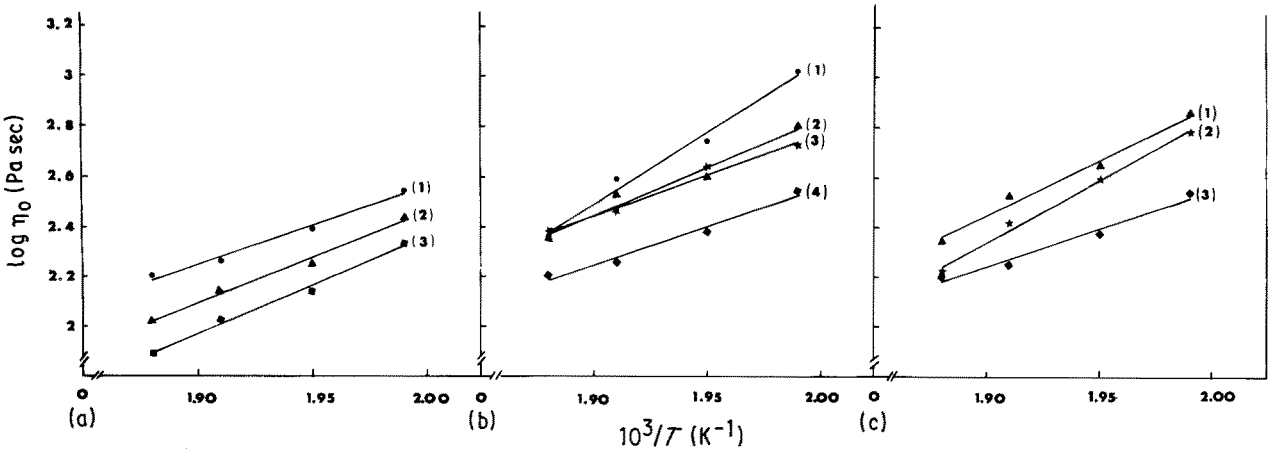

Figure 2 Dependence of the logarithm of zero shear viscosity, log η_0, on the reciprocal absolute temperature, $1/T$, for plain PA6 and PA6/EVA blends. (a) 1, PA6/EVA5 90/10; 2, PA6/EVA2 90/10; 3, PA6/EVA 100/0. (b) 1, PA6/EVA7 90/10; 2, PA6/EVA6 90/10; 3, PA6/EVA4 90/10; 4, PA6/EVA 100/0. (c) 1, PA6/EVA 100/0; 2, PA6/EVA3 90/10; 3, PA6/EVA1 90/10.

closely approach that of pure PA6. This finding, according to the results reported in a previous paper [2], confirms that PA6 and EVA copolymers are incompatible in the molten state.

As may be expected, the X_c(blend) values are found to be lower than that of pure PA6; no systematic dependence on the type of EVA copolymer added is found. The X_c values of the PA6 phase crystallized in the presence of EVA copolymers are quite comparable to that of pure PA6.

3.2. Melt rheology

Fig. 1 shows the dependence of the logarithm of the apparent viscosity, η_a, on the logarithm of shear rate, $\dot{\gamma}$, for plain PA6 and PA6/EVA blends. As can be observed, both PA6 and PA6/EVA show pseudoplastic behaviour, whereby the apparent viscosity, η_a, decreases as the rate of shear increases over the whole range of temperatures and shear rate investigated.

The shear dependence of the viscosity was analysed by using a modified Cross–Bueche equation [10]

$$\eta_0/\eta_a = 1 + (\alpha\dot{\gamma})^m \quad (1)$$

where η_0 is the zero-shear viscosity, α is a parameter which according to Cross [11] should correspond to the characteristic relaxation time, and m gives a measure of the shear-thinning of the melt, i.e. a measure of the decrease in viscosity with increasing rate of shear. For polymers with a distribution of molecular weights, Cross [11] claims that $m = (\bar{M}_n/\bar{M}_w)^{1/5}$. According to Iwakura and Fujimura [12] α is related to the size of the apparent flow unit; the reciprocal of α corresponds to the shear rate at which $\eta_a = \eta_0/2$.

Plots of $1/\eta_a$ against $\dot{\gamma}^m$ for plain PA6 are linear for $m = 8/9$ (usually linearity is obtained with a lower m value ($m = 2/3$) [13]) indicating a severe shear thinning in the non-Newtonian region; on the other hand, the PA6/EVA blends show linearity in the plot $1/\eta_a$ against $\dot{\gamma}^m$ for $m = 2/3$. From the plots of $1/\eta_a$ against $\dot{\gamma}^m$, the zero-shear viscosity, η_0 and α are easily obtained from the reciprocal of the intercept and from the slope, respectively.

The η_0 and α values of pure PA6 and its blends with EVA copolymers over the whole range of temperatures investigated are reported in Table III. As shown, for all samples investigated the η_0 and α values decrease with increasing temperature. It should be noted, moreover, that the zero-shear viscosity values of the blends containing the copolymers having low molecular mass (EVA1 and EVA3) are lower than those of plain PA6. On the other hand, all the remaining blends show η_0 values higher than those of PA6.

The α values obtained for pure PA6 are always lower than those of PA6/EVA blends. As the reciprocal of the parameter α corresponds to the shear rate at which η decreases to half of η_0, shorter α values mean that the non-Newtonian flow starts at a higher shear rate. Thus the range of the Newtonian behaviour of the pure PA6 is to be expected larger than that of blends for which the transition from the Newtonian to pseudoplastic flow seems to begin at lower $\dot{\gamma}$ values. Such findings are in qualitative agreement with the results obtained by Utraki and Kamal [14], and Han *et al.* [15] in the case of incompatible polymer blends.

At a given temperature, a comparison between the data listed in Table III seems to indicate that in the case of blends both η_0 and α increase with increasing (i) the molecular mass of the copolymers (for a given percentage of vinyl acetate), and (ii) the percentage of vinyl acetate of the copolymer (for a given molecular mass). For both PA6 and PA6/EVA blends, plots of log η_0 against the reciprocal of the temperature are straight lines (Fig. 2). Thus, the temperature dependence of the viscosity may be accounted for by an exponential relation of the type [16]

$$\eta_0 = A \exp(\Delta E^*/(RT)) \quad (2)$$

TABLE IV Activation energy (ΔE^*) values of plain polyamide 6 (PA6) and PA6/ethylene–vinyl acetate copolymer (EVA) blends

Code	ΔE^* (10^3 J mol^{-1})
PA6	26.02
PA6/EVA1	32.34
PA6/EVA2	42.22
PA6/EVA3	30.10
PA6/EVA4	27.65
PA6/EVA5	36.90
PA6/EVA6	31.67
PA6/EVA7	47.66

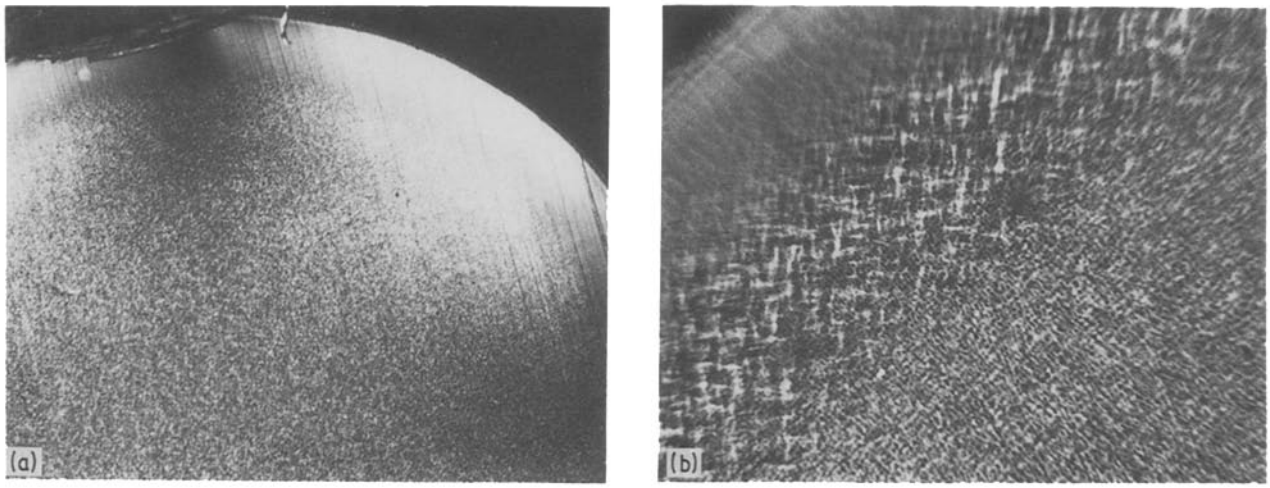

Figure 3 Optical micrographs with crossed polars of a thin transverse section of plain PA6 filaments: (a) ×44, (b) ×224.

where A is a constant and ΔE^* is the activation energy for the viscous flow.

As shown in Table IV, ΔE^* values of the blends are higher than that of plain PA6 with no systematic dependence upon the molecular mass and vinyl acetate content of the copolymers; the highest value is obtained in the case of PA6/EVA7 blends. The observed increase in ΔE^* values of the blends could indicate a growth of the volume of the flow element. Such findings tend to support the flow model of melts for incompatible blends proposed by Utraki and Kamal [14]. By adding EVA copolymer to the PA6 homogeneous melt, the initial EVA dispersion in the form of readily deformable droplets generates a series of shear-dependent structures, each with its own value of the characteristic zero-shear viscosity, that have to be destroyed before the molecules of the PA6 matrix can flow.

In principle at least the presence of some kind of association between the two types of macromolecule cannot be excluded.

3.3. Phase morphology transverse to the flow direction

As already reported [17], thin transverse sections, cut from plain PA6 filaments and observed by means of an optical microscope with crossed polars, show a skin–core morphology (Fig. 3). Going from the border to the interior the following different morphological structures of PA6 are progressively found: a skin, about 15 μm thick, having spherulitic superstructure, a birefringent transcrystalline layer about 100 μm thick, resulting from a localization of nuclei that greatly distort spherulitic growth [7], an inner granular non-spherulitic structure about 70 μm thick, and a spherulitic core. The development of such morphologies probably results from a combination of flow pattern, supercooled melts and the presence of solid impurities.

By adding EVA copolymers, irrespective of their molecular characteristics, the PA6 skin–core morphology disappears. As shown by Fig. 4, a homogeneous spherulitic superstructure over the whole transverse sections of PA6/EVA filaments is observed. The analysis of the EVA state of dispersion carried out by SEM in the core of transverse surfaces of cryogenically fractured samples shows that the minor component segregates in spherical-shaped domains. Moreover, no morphological evidence of adhesion at the interface between matrix and dispersed phase is found. On the walls of the cavities, left by the EVA particles jumping during the fracture, the PA6

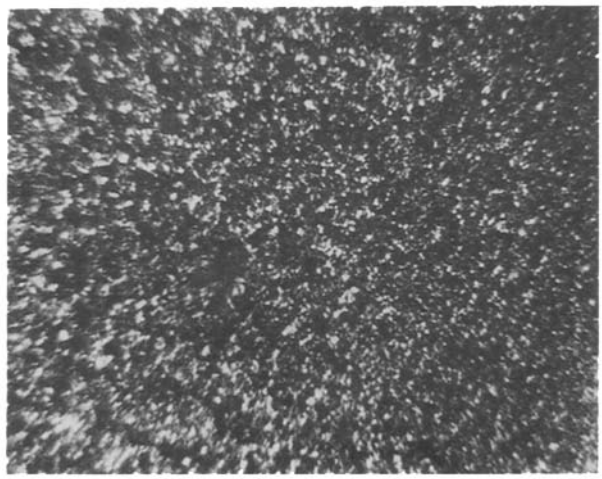

Figure 4 Optical micrographs with crossed polars of a thin transverse section of the PA6/EVA1 blend, 20% vinyl acetate, border area, ×225.

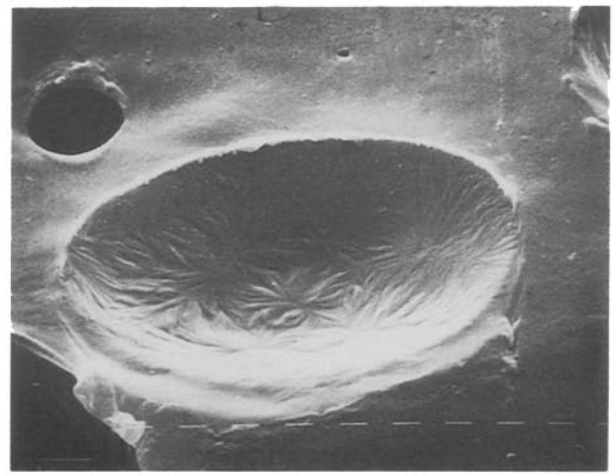

Figure 5 Scanning electron micrographs of smoothed surfaces of PA6/EVA1 blend, 20% vinyl acetate, exposed to boiling xylene vapour, ×3500.

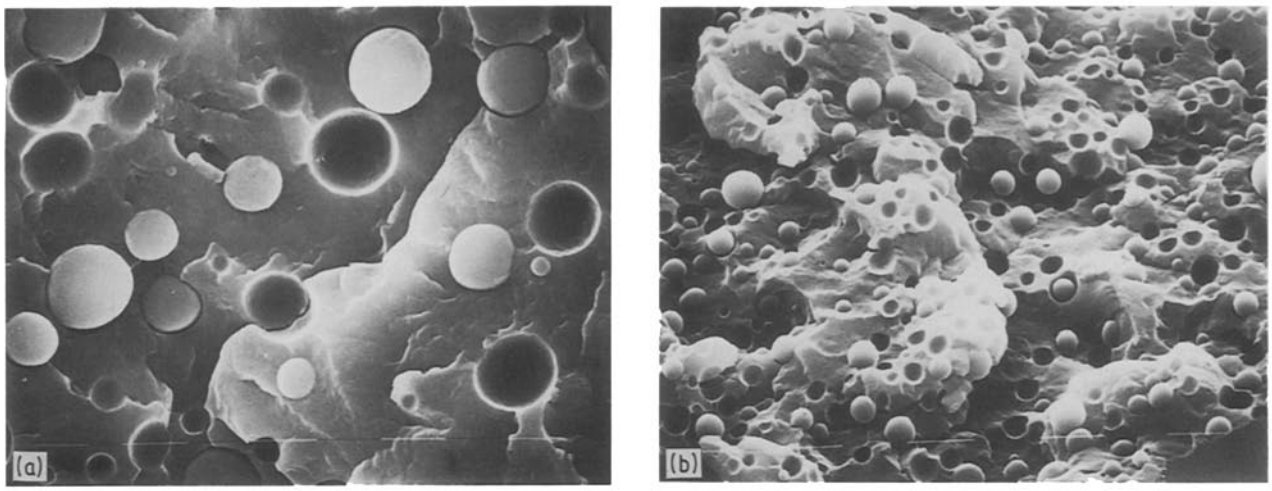

Figure 6 Scanning electron micrographs of cryogenic fracture surfaces of the blends with 20% vinyl acetate, core area: (a) PA6/EVA1, ×889; (b) PA6/EVA2, ×889.

spherulites are clearly visible (see Fig. 5). It is interesting to note that the size of the EVA domains is strongly dependent upon the chemical and molecular characteristics of the copolymers.

In the case of the blends containing the copolymers having 20% (wt/wt) vinyl acetate along their chain (EVA1 and EVA2) the SEM investigation shows that a finer morphology is developed in EVA2-containing blends. As a matter of fact, in such a blend the EVA2 copolymer domains have a diameter ranging between 2.0 and 7.0 μm whereas in EVA1-containing blends the range of results is wider (2.0 up to 14.0 μm; cf. Figs 6a and b). These morphological results suggest that the primary factor in determining the dispersion coarseness of EVA copolymers containing the same vinyl acetate percentage (wt/wt) could be their melt viscosity. The higher the melt viscosity (see Table I), the smaller are the EVA particles (see Figs 6a and b).

In EVA3-, EVA4- and EVA5-containing blends, the particle size of the dispersed phase is contained in the following ranges: 2.0 to 14.0 μm (EVA3) and 0.8 to 4.0 μm (EVA4 and EVA5) (see Fig. 7). By comparing such ranges, it emerges clearly that a finer dispersion of the minor component in the EVA4- and EVA5-containing blends is achieved. As EVA3, EVA4 and EVA5 copolymers contain the same vinyl acetate percentage (wt/wt), the degree of dispersion (average particle size) seems to be determined by their melt viscosity. In agreement with the results obtained in the case of EVA1- and EVA2-containing blends, finer dispersion of the minor component is developed in blends containing copolymers with comparatively higher molecular mass.

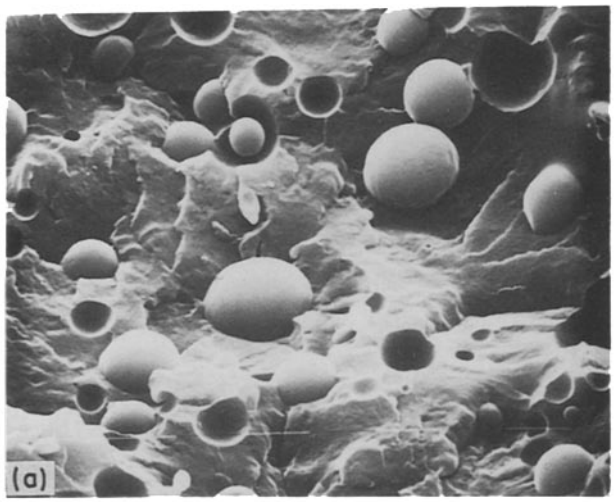

Figure 7 Scanning electron micrographs of cryogenic fracture surfaces of the blends with 30% vinyl acetate, core area: (a) PA6/EVA3, ×940; (b) PA6/EVA4, ×940; (c) PA6/EVA5, ×940.

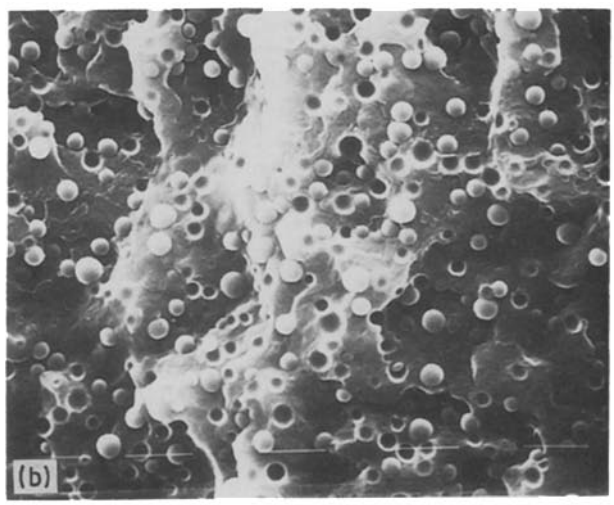

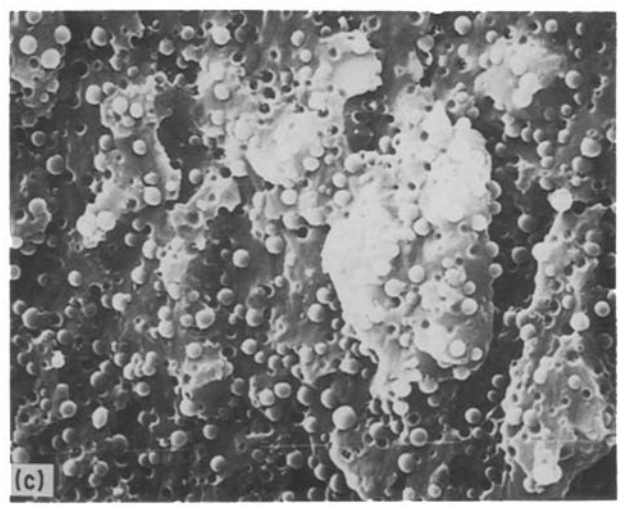

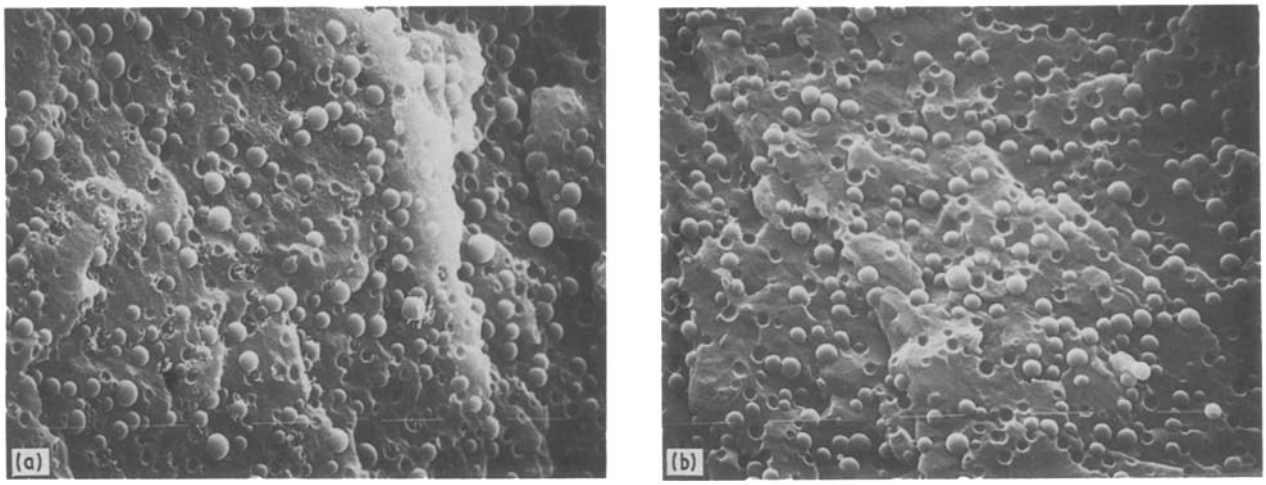

Figure 8 Scanning electron micrographs of cryogenic fracture surfaces of the blends, core area: (a) PA6/EVA6, 35% vinyl acetate, ×874; (b) PA6/EVA7, 40% vinyl acetate, ×874.

Looking at the influence of vinyl acetate content on the state of dispersion of EVA1, EVA3 and EVA2, EVA5 copolymers it emerges that increasing the vinyl acetate content from 20% (wt/wt) to 30% (wt/wt) along the copolymer chain, the range of EVA1 and EVA3 particle size remains unaffected (compare Figs 6a and 7a). On the other hand, the range of EVA5 particle size is sharper than that shown by EVA2 (compare Figs 6b and 7c). Such morphological results seem to support the hypothesis that the main factor in determining the coarseness of the dispersion of EVA copolymers in the PA6 matrix could be their melt viscosity. The vinyl acetate content seems to play a second role as an increase in such content along the copolymer chain seems to promote finer dispersion of the minor component only in the case of the copolymer having a higher melt viscosity (EVA5) (see Table I).

Scanning electron micrographs of cryogenically fractured filaments of EVA6- and EVA7-containing blends are shown in Fig. 8. Irrespective of the vinyl acetate content (see Table I), a fine dispersion in both cases is developed. The EVA particles have, in fact, a diameter ranging between 0.8 and 4.0 μm. Note that the degree of dispersion achieved in EVA6- and EVA7-containing blends is quite comparable to that obtained in EVA4- and EVA5-containing blends.

Contrary to expectation, a vinyl acetate increase above 30% (wt/wt) along the EVA copolymer chain does not induce a reduction in the particle size of the dispersed phase (compare Figs 7c and 8). The morphological analysis by SEM of the EVA mode of dispersion, performed on smoothed surfaces of PA6/EVA filaments exposed to boiling xylene vapour shows an anisotropic distribution of the dispersed phase (see Fig. 9). In fact, the EVA particle size increases going from the skin towards the core of the filaments with a gradient characteristic. Note that the gradient in particle size increases with increasing mean size of the EVA domains in the centre of the filaments (see Fig. 10). This phenomenon would appear to be due to the higher stress occurring in the outer regions of the filaments during the extrusion.

Figure 9 Scanning electron micrographs of smoothed surfaces exposed to boiling xylene vapour of the PA6/EVA1 (90/10) blend, 20% vinyl acetate ×58.

3.4. Phase morphology longitudinal to the flow direction

The morphological analysis by SEM performed on longitudinal cryogenic fracture surfaces of PA6/EVA blends shows that in the regions closer to the border of the filaments the EVA droplets become more or less elongated along the flow direction. The remaining samples show a droplet-like morphology of the dispersed phase. The observed deformation of the particle shape may probably to be ascribed to the higher shear stress occurring in the outer regions of the filaments. It should be noted that ellipsoidal and/or cylindrical shaped domains are observed depending on the chemical and molecular characteristics of the dispersed phase.

From analysis of the extent of the deformation undergone by domains of copolymers having the same melt viscosity it emerges that in the case of the blends containing a copolymer having comparatively higher melt viscosity (EVA2 and EVA5), the EVA2 copolymer forms fibrils parallel to the flow whereas the EVA5 droplets become slightly deformed (compare Figs 11a and 12a, 11b and 12b).

It must be kept in mind that the average particle sizes of the EVA2 and EVA5 dispersed particles are 4.5 and 2.4 μm, respectively. As shown in Figs 13a and

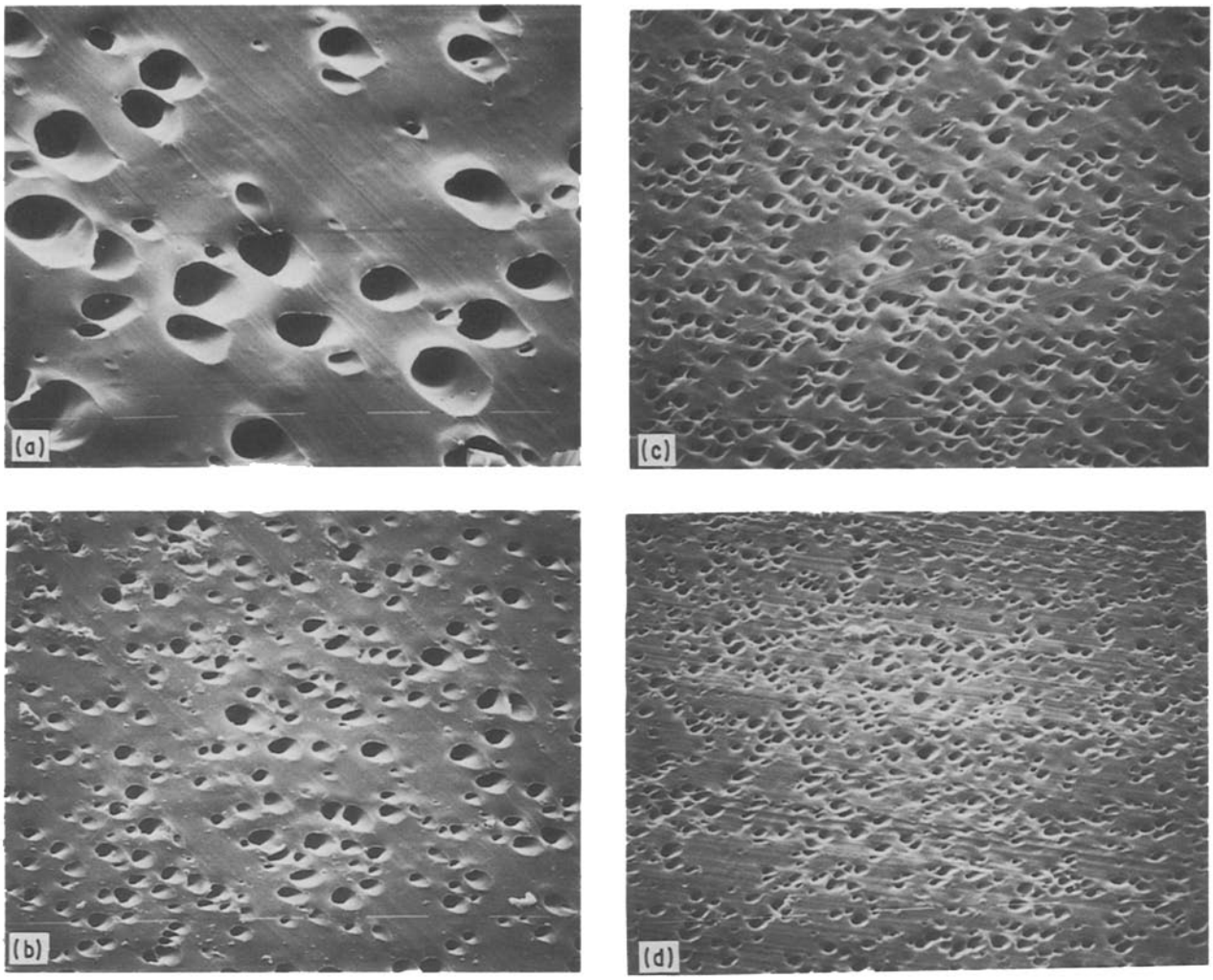

Figure 10 Scanning electron micrographs of smoothed surfaces exposed to boiling xylene vapour of the blends PA6/EVA3, 30% vinyl acetate (a) core, ×885, (b) border, ×885, and PA6/EVA7, 40% vinyl acetate (c) core, ×885, (d) border, ×885.

b, the spherical-shaped domains of EVA4, EVA6 and EVA7 copolymers having intermediate melt viscosities (see Table I) exhibit a resistance to deformation by shear stress quite comparable to that shown by EVA5 droplets (compare Figs 13a, b and 11b). It is interesting to note that the copolymers EVA4, EVA5, EVA6 and EVA7 segregate in particles having the same average dimensions (2.4 μm). Looking at the longitudinal mode of dispersion in the regions close to the border of filaments of blends containing EVA1 and EVA3 copolymers having comparatively lower molecular mass (see Table I), it can be seen that EVA1 droplets assume an ellipsoidal shape whereas EVA3 particles become both ellipsoidal and cylindrical (compare Figs 14a and b). As previously reported, the average particle size of both such copolymers is about 8.0 μm.

All the above results seem to indicate that:

(i) in the outer regions of the filaments only particles larger than 4.0 μm are considerably deformed by shear stress. Such a finding seems to suggest that the particle radius could be the main factor in determining the droplet formation;

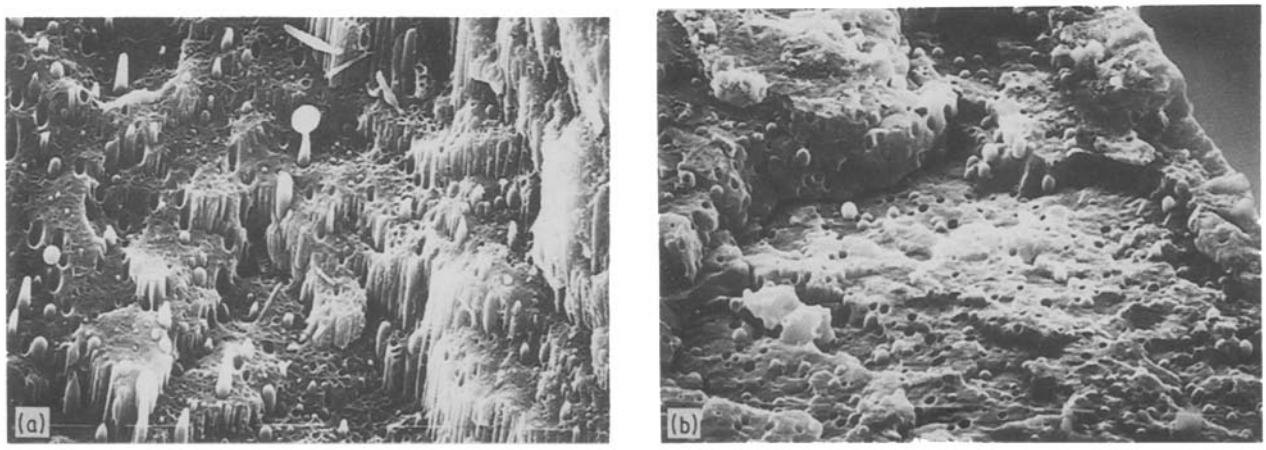

Figure 11 Scanning electron micrographs of longitudinal cryogenic fracture surfaces of the blends, border area (a) PA6/EVA2, 20% vinyl acetate, ×925, (b) PA6/EVA5, 30% vinyl acetate, ×925.

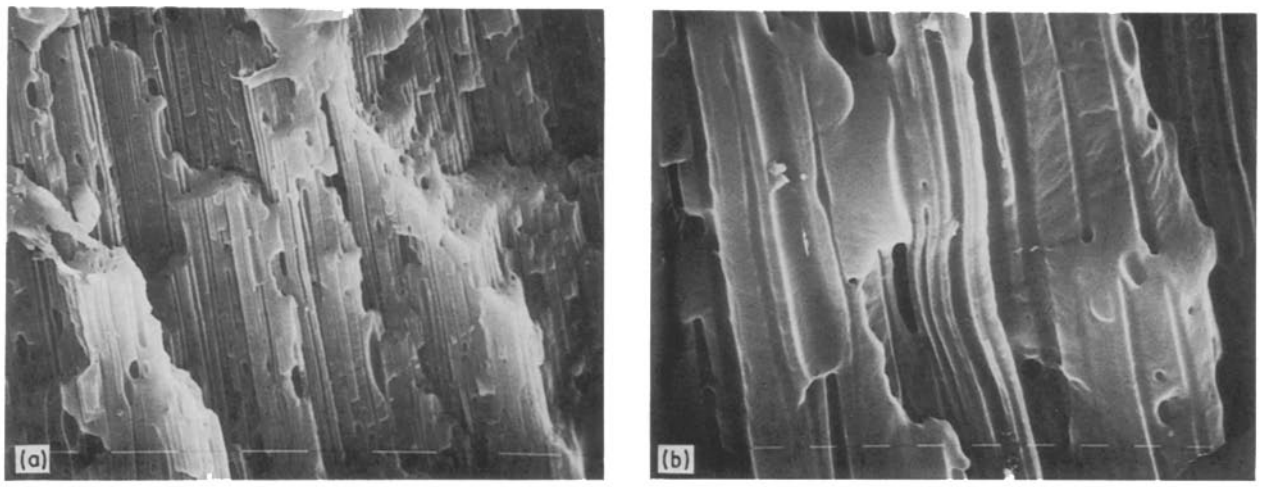

Figure 12 Scanning electron micrographs of longitudinal cryogenic fracture surfaces exposed to boiling xylene vapour of the PA6/EVA2 blend, 20% vinyl acetate, border area: (a) ×874, (b) ×3612.

(ii) the extent of deformation depends on the melt viscosity of the minor component. The higher the melt viscosity, the greater is the deformation undergone.

3.5. Rheology–structure relationships

The morphologies transverse to the flow direction of PA6/EVA blends are summarized in Table V together with the zero-shear viscosity, η_0, values, the characteristic relaxation time, α, values calculated at the extrusion temperature (240° C) using a modified Cross equation [10] and the molecular characteristics of EVA copolymers.

Examining the observed rheological behaviour of such blends from the point of view of the mode and state of dispersion of the minor component, it can be seen that blends, in which EVA coarser dispersion is developed (PA6/EVA1 and PA6/EVA3), show η_0 values lower than that of both plain PA6 and the remaining blends. On the other hand, η_0 values higher than that of pure PA6 are exhibited by blends showing a finer dispersion of the minor component (see Tables III and V). It is interesting to observe, moreover, that the blend α values increase with decreasing particle size of discrete phase (see Table V). Such a finding suggests that for blends, in which a finer dispersion of EVA copolymer is developed, the transition from the Newtonian to pseudoplastic flow starts at lower $\dot{\gamma}$ values.

Comparatively higher η_0 and α values are shown by blends containing the copolymer EVA7 having intermediate molecular mass and the highest content of vinyl acetate along its chain.

In the absence of flow, the scale of dispersion coarseness of the discrete phase is associated with the interfacial tension, keeping the suspended phase in the shape of spheres. Thus a coarser dispersion, lowever η_0 and α values could be related to higher interfacial forces. It should also be noted that:

(i) higher η_0 and α values and smaller particle size are exhibited by blends containing EVA copolymers with comparatively higher molecular mass (for a given vinyl acetate content along EVA chains);

(ii) for higher EVA molecular mass, increasing the vinyl acetate content along the copolymer chain from 20% up to 30% (wt/wt), an increase in the blend η_0 and α values and a decrease in particle size are observed. No systematic increase in η_0 and α values and no further reduction in particle size in the case of the blends containing copolymer with a vinyl acetate content higher than 30% (wt/wt) are observed.

4. Concluding remarks

A study of the melt rheology and of the development of phase morphology during extrusion of PA6-based blends, containing several EVA copolymers differing in molecular mass and for a given molecular mass in the vinyl acetate content, has been reported. Certain trends are clear.

1. The zero-shear viscosity (η_0) values of PA6/EVA blends, calculated using a modified Cross–Bueche equation [10], were found to be mainly dependent on molecular mass of EVA copolymers. Over the whole range of temperatures explored, the η_0 values of blends containing copolymer with low molecular mass were

TABLE V Range of particle size, zero-shear viscosity, η_0, and characteristics relaxation time, α, at extrusion temperature (240° C) for polyamide 6 (PA6)/ethylene–vinyl acetate copolymer (EVA) blends

Sample	Range of particle size (μm)	η_0 (Pa sec)	α (10^{-3} sec)	Melt index (g 10 min^{-1})	% vinyl acetate (wt/wt)
PA6/EVA4	0.8–4	433.2	3.83	30–40	30
PA6/EVA5	0.8–4	441.6	3.39	3–4	30
PA6/EVA6	0.8–4	395.6	3.30	30–40	35
PA6/EVA7	0.8–4	549.3	5.77	30–40	40
PA6/EVA2	2.0–7	401.8	2.91	3–4	20
PA6/EVA1	2.0–14	140.9	0.820	300–500	20
PA6/EVA3	2.0–14	177.0	1.10	300–500	30

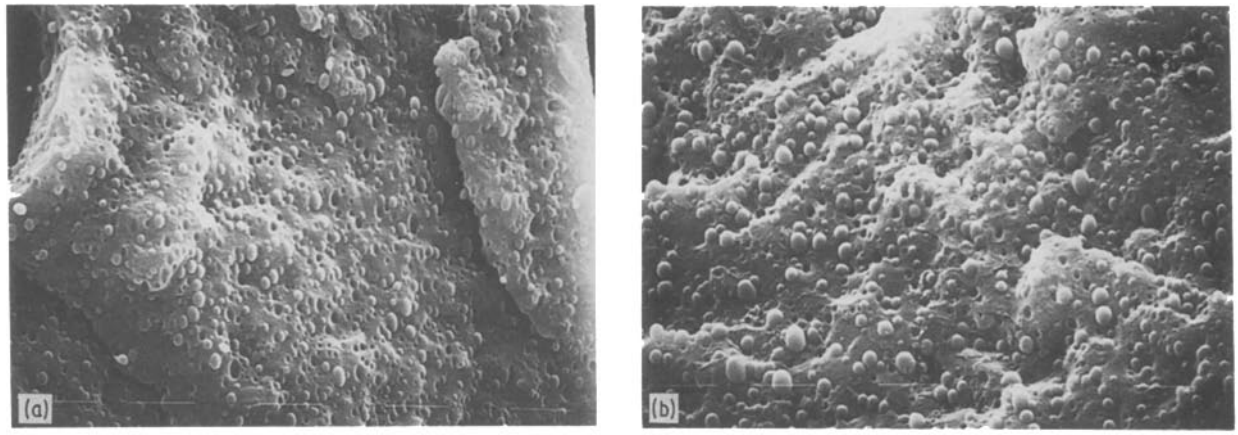

Figure 13 Scanning electron micrographs of longitudinal cryogenic fracture surfaces of the blends, border area: (a) PA6/EVA4, 30% vinyl acetate, ×900, (b) PA6/EVA7, 40% vinyl acetate, ×900.

found to be lower than that of plain PA6, whereas higher η_0 values are shown by all the remaining blends. The values of characteristic relaxation time, α, for PA6 were always lower than those of PA6/EVA blends. Such a finding, in agreement with the results obtained by Utraki and Kamal [14] and Chuang and Han [4] in the case of incompatible polymer blends, indicates that for the blends the transition from the Newtonian to pseudoplastic flow starts at $\dot{\gamma}$ values lower than that of plain PA6. It was also observed that, at a given temperature, both blend η_0 and α values increase with increasing (i) the molecular mass of the copolymers for a given percentage of vinyl acetate, and (ii) the percentage of vinyl acetate of the copolymer for a given molecular mass.

The activation energy for the viscous flow ΔE^* values calculated for PA6/EVA blends was found to be higher than that of plain PA6, indicating a growth of the volume of the flow element and supporting the flow model of melts of incompatible blends proposed by Utraki and Kamal [14].

2. The EVA minor component segregated mainly in spherical-shaped domains with no morphological evidence of adhesion at the interface between PA6 matrix and dispersed phase. The order of dispersion coarseness of the minor component is mainly determined by EVA melt viscosity. For a given content of vinyl acetate along the EVA chain, a finer dispersion was developed in blends containing copolymers with comparatively higher molecular mass. For a given EVA molecular mass, an increase of vinyl acetate content along the copolymer chain from 20% (wt/wt) to 30% (wt/wt) promotes finer EVA dispersion only in the case of the copolymer having a higher melt viscosity. It should also be noted that a vinyl acetate increase of more than 30% (wt/wt) along the EVA chain does not induce a further reduction in particle size of the dispersed phase.

Smoothed surfaces of PA6/EVA filaments exposed to boiling xylene vapour also showed an anisotropic distribution of dispersed phase. The EVA particle size was found to increase going from the skin towards the core of the filaments with a gradient characteristic. This phenomenon would appear to be due to the higher stress occurring in the outer regions of the filaments during extrusion.

In the outer regions of the filaments, ellipsoidal and/or cylindrical shaped domains were observed. The deformation undergone was found to be mainly dependent on the particle radius because only droplets larger than 4.0 μm were elongated by shear stress. The extent of deformation was determined by the melt viscosity of the EVA minor component. The higher the melt viscosity, the higher was the deformation undergone.

3. The rheological behaviour of PA6/EVA blends was correlated with the mode and state of EVA dispersion developed during extrusion. It was found that the

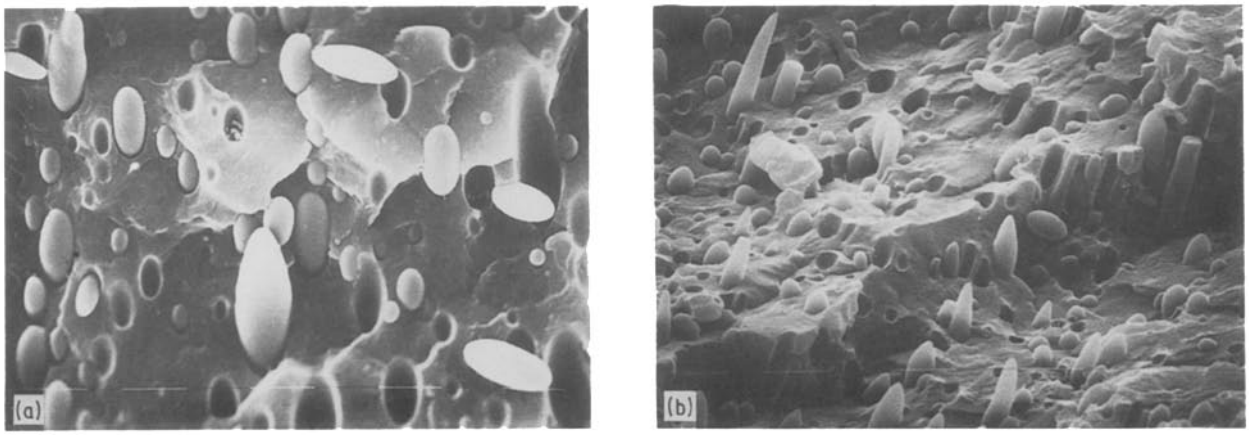

Figure 14 Scanning electron micrographs of longitudinal cryogenic fracture surfaces of the blends, border area: (a) PA6/EVA1, 20% vinyl acetate, ×900, (b) PA6/EVA3, 30% vinyl acetate, ×900.

scale of dispersion coarseness of the minor component may greatly influence the rheological properties of such incompatible blends. Larger droplets were developed in blends showing lower η_0 and α values. Such findings suggest that the particle size of the suspended phase could determine the $\dot{\gamma}$ values for which the transition from the Newtonian to pseudoplastic flow starts.

References

1. L. D'ORAZIO, C. MANCARELLA, E. MARTUSCELLI, A. CASALE, A. FILIPPI and F. SPERONI, *J. Mater. Sci.* **21** (1986) 989.
2. *Idem, ibid.* **22** (1987) 429.
3. CHANG DAE HAN and HSIAO-KEN CHUANG, *J. Appl. Polym. Sci.* **30** (1985) 2431.
4. HSIAO-KEN CHUANG and CHANG DAE HAN, *ibid.* **30** (1985) 165.
5. SOUHENG, WU, *Polymer* **26** (1985) 1855.
6. S. CIMMINO, L. D'ORAZIO, R. GRECO, G. MAGLIO, M. MALINCONICO, C. MANCARELLA, E. MARTUSCELLI, R. PALUMBO and G. RAGOSTA, *Polym. Engng Sci.* **24** (1984) 48.
7. M. I. KOHAN, "Nylon Plastics" (Wiley, New York, 1973) p. 329.
8. M. DOLE and B. WUNDERLICH, *Makromol. Chem.* **34** (1959) 29.
9. A. M. REIMSCHUESSEL, *J. Polym. Sci. Macromol. Rev.* **12** (1977) 65.
10. T. FUJIMURA and K. IWAKURA, *Int. Chem. Engng* **10** (1970) 683.
11. M. M. CROSS, *J. Appl. Polym. Sci.* **13** (1969) 765.
12. K. IWAKURA and T. FUJIMURA, *ibid.* **19** (1975) 1427.
13. M. M. CROSS, *J. Colloid Sci.* **20** (1965) 417.
14. L. A. UTRAKI and M. R. KAMAL, *Polymer Engng Sci.* **22** (1982) 96.
15. C. D. HAN, K. U. KIM, J. PARKER, N. SISKOVIC and C. R. HUANG, *Appl. Polym. Symp.* **20** (1973) 191.
16. D. W. VAN KREVELEN, "Properties of Polymers" (Elsevier Scientific, New York, 1976).
17. S. S. KATTI and J. M. SCHULTZ, *Polym. Engng Sci.* **22** (1982) 1001.

Received 6 May
and accepted 9 September 1988